Infrared and Raman Spectroscopic Studies on Alkali Borate Glasses: Evidence of Mixed Alkali Effect

G. Padmaja and P. Kistaiah*

Department of Physics, Osmania University, Hyderabad 500 007, India

Received: October 21, 2008; Revised Manuscript Received: January 9, 2009

A lithium−potassium−borate glass system containing manganese and iron cations has been thoroughly investigated in order to obtain information about the mixed alkali effect and the structural role of both the manganese and iron in such glass hosts. Mixed alkali borate glasses of the $(30 - x)Li_2O - xK_2O - 10CdO/ZnO - 59B_2O_3$ ($x = 0$, 10, 15, 20, and 30) doped with $1MnO_2/1Fe_2O_3$ system were prepared by a melt quench technique. The amorphous phase of the prepared glass samples was confirmed from their X-ray diffraction. The spectroscopic properties of glass samples were studied using infrared (IR) and Raman spectroscopic techniques. The density of all the prepared glasses was measured using Archimedes principle. Molar volumes were estimated from the density data. IR spectra of these glasses revealed a dramatic variation of three- and four-coordinated boron structures as a function of mixed alkali concentration. The vibrations due to Li−O, K−O, and MnO_4/FeO_4 arrangements are consistent in all the compositions and show a nonlinear variation in the intensity with alkali content. Raman spectra of different alkali combinations with CdO and ZnO present drastic changes in the intensity of various Raman bands. The observation of disappearance and reappearance of IR and Raman bands as a function of various alkali concentrations is an important result pertaining to the mixed alkali effect in borate glasses. Acting as complementary spectroscopic techniques, both types of measurements, IR and Raman, revealed that the network structure of the studied glasses is mainly based on BO_3 and BO_4 units placed in different structural groups, the BO_3 units being dominant. The measured IR and Raman spectra of different glasses are used to clarify the optical properties of the present glasses correlating them with their structure and composition.

1. Introduction

Alkali borate glasses are an important class of solid materials for various technological applications such as solid electrolytes, insulation materials, textile fiber glass, etc. These materials have been under intense research to understand the structural and physical properties through various experimental techniques. Observation of nonlinear behavior in various physical properties including viscosity, chemical durability, alkali diffusion, electrical conductivity, mechanical relaxation, and spectroscopic parameters, with systematic doping of one alkali ion with another, has emerged as an interesting phenomenon referred to as the "mixed alkali effect" (MAE).[1−3] MAE has been observed in various glassy systems such as borosilicate glasses, phosphate glasses, and borate glasses. The mixed alkali phenomenon from a practical viewpoint is useful in manufacturing low-loss electrical glass and in understanding chemical strengthening of glass.[3−5] However, MAE is still an open question in this area. Few models are developed to explain this effect, depending on both structural and electrodynamic theories.[6−9] No single model however seems to provide a satisfactory explanation of the mixed alkali effect on diverse systems. In studying the mixed alkali effect therefore one generally considers factors specific to the particular glass system being investigated.

Boron oxide-based glasses exhibit rich structural chemistry of structure. Boron is commonly three- or four-coordinated with oxygen, and these coordinations are exhibited in a wide variety of borate glasses and minerals.[10] The addition of modifier oxides such as alkali, alkaline earth, and transition oxides to borate glasses suggests that there will be local configurational changes in the glass network in addition to an increase in the number of free carriers.[11] Addition of various alkali modifiers, A_2O (A: Li, Na, K, Rb, Cs), to the borate glasses brings drastic changes in the structural units. The structure of glassy alkali borates is a complex three-dimensional network of boron and oxygen composed of larger structural units. These structural units are sketched in Figure 1.[12] The added modifier can act in two different ways: by forming four-coordinated boron (BO_4^-)

$$2(BO_3) \xrightarrow{A_2O} 2(BO_4^-) + 2A^+ \quad (1)$$

and by forming nonbridging oxygen (NBO)

$$2(BO_3) \xrightarrow{A_2O} 2(BO_3^-) + 2A^+ \quad (2)$$

In reaction 1, all of the oxygen atoms are bridging atoms between boron atoms. In reaction 2, one of the oxygen atoms in each of the BO_3^- units is nonbridging. The existence of four-coordinated boron in alkali-doped borate glasses has been studied extensively for a wide variety of modifiers through various spectroscopic techniques such as IR, Raman, NMR, and NQR spectroscopy.[13−15] The concentration of four-coordinated boron in modified borate networks is dominant below 30% added modifier and reaction 1 plays vital role in this region. Above 30% added modifier content, reaction 2 is dominant and

* Corresponding author: pkistaiah@yahoo.com.

10.1021/jp809318e CCC: $40.75
Published on Web 02/23/2009

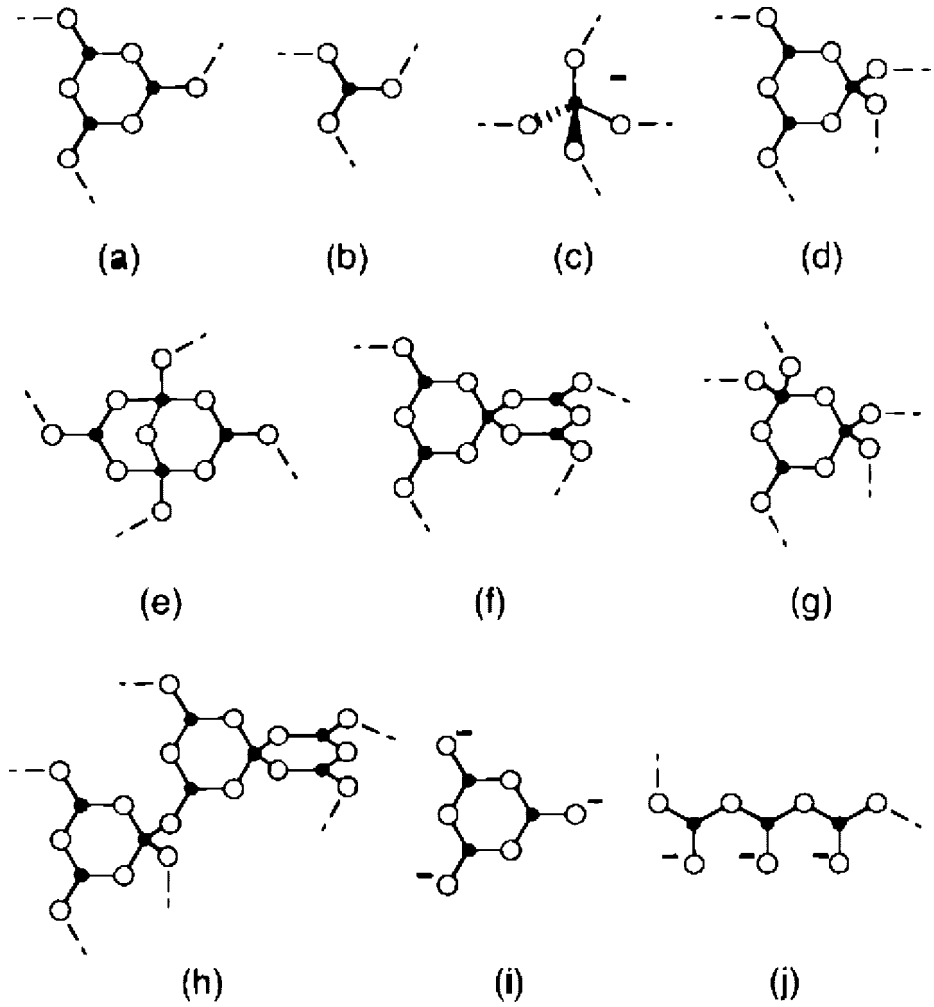

Figure 1. Possible structural groups found in alkali borate glasses: (a) boroxol ring, (b) nonring BO_3, (c) nonring BO_4^-, (d) triborate, (e) diborate, (f) pentaborate, (g) di-triborate, (h) tetraborate, (i) ring-type metaborate, and (j) chain-type metaborate. Filled circles and open circles represent boron and oxygen atoms, respectively. Dashed lines in the structures denote connections to the network, and charges are shown for the nonbridging oxygen (NBO) in the metaborate groups.

NBO formation is more than four coordinated borons in the glass network. There were several systematic studies to quantify the concentration of four-coordinated boron and NBOs in understanding the structure of modified glasses. Magnetic resonance has been extensively used and successful in mapping these structural changes in modified glasses. Bray and co-workers inferred the existence of multiple three- and four-coordinated boron sites in their ^{11}B NMR spectra.[16] In contrast to magnetic resonance experiments, Raman spectroscopy can detect larger structures involving several atoms and can be used to monitor changes in glass networks. Raman spectroscopic studies on alkali oxide-doped borate glasses clearly show gradual emergence of Raman bands between 740 and 780 cm^{-1} which replace the 808 cm^{-1} band. This has been attributed to the conversion of the boroxol rings to other ring-type structures containing four-coordinate boron. Owing to the disorder of the glasses, assignment of Raman bands is made by comparison with the spectral features of crystalline alkali borates. In IR spectra B−O stretching and B−O−B bending frequencies would be affected by any such structural changes. The IR spectra of glasses provides significant information of various bonds present between different ions in the glass network and these are identified by comparing the experimental data of glasses with those of related crystalline compounds.[17,18]

Multicomponent glasses are technologically important, as the properties of these glasses can be engineered to achieve desired properties. The mixed alkali effect in these glass systems explores chances of tailoring properties. Interestingly the addition of transition element also modifies the structural units and in some cases the transition elements behave like network builders instead of behaving like modifiers. The present investigation is intended to establish aspects related to the preparation conditions and structure of a more complex multicomponent glass system $Li_2O-K_2O-CdO/ZnO-B_2O_3$ doped with MnO_2/Fe_2O_3 transition metal ions by means of two complementary spectroscopic methods, infrared absorption and Raman scattering. X-ray diffraction was used to obtain information about the short-range order structure of these glasses.

2. Experimental Section

The glass systems with the compositions $(30 - x)Li_2O - xK_2O - 10CdO/ZnO - 59B_2O_3$ ($x = 0$, 10, 15, 20, and 30) doped with $1MnO_2$ (LKCBM/LKZBM) and $1Fe_2O_3$ (LKCBF/LKZBF) were prepared through a melt and quenching technique. The compositions of various glass samples prepared in this study are presented in Table 1. All the glass compositions were prepared by mixing stoichiometric amounts of pure reagent grade compounds; i.e., Li_2CO_3, K_2CO_3, $CdCO_3$, ZnO, MnO_2, Fe_2O_3, and H_3BO_3. The mixed precursor powders were melted at 1273 K for 30 min and quenched to room temperature in air. The prepared glasses were annealed for 4 h at 623 K to remove

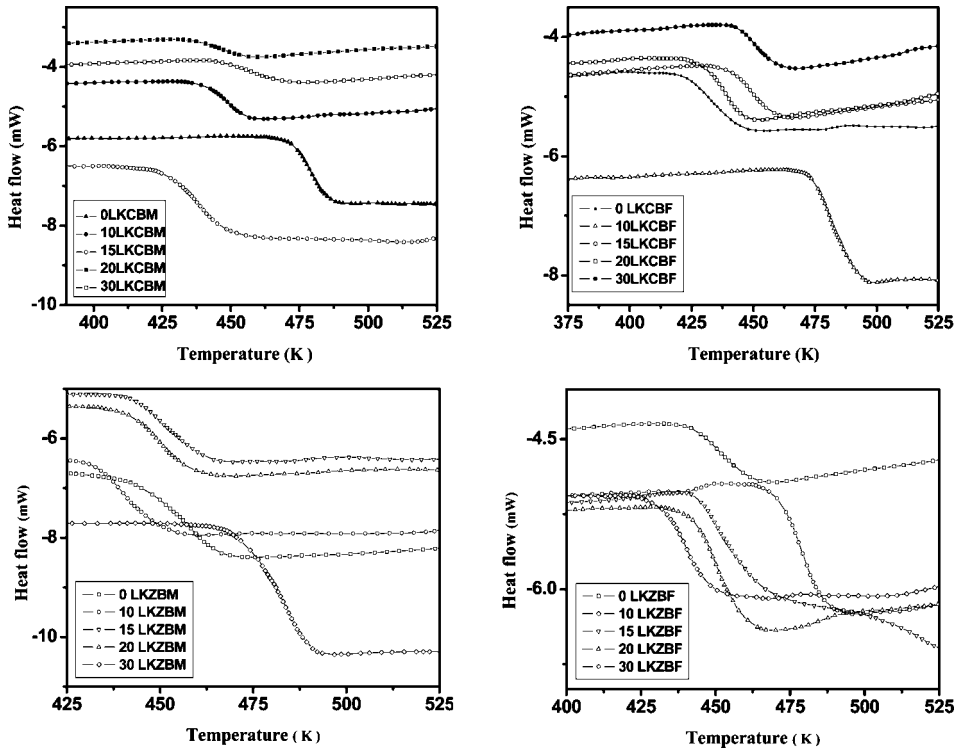

Figure 2. DSC patterns of LKCBM, LKCBF, LKZBM, and LKZBF glasses.

TABLE 1: Compositions (%) of Various Oxide Materials in the Studied Glasses

Mn series	Li_2O	K_2O	CdO	B_2O_3	MnO_2
0LKCBM	30	0	10	59	1
10LKCBM	20	10	10	59	1
15LKCBM	15	15	10	59	1
20LKCBM	10	20	10	59	1
30LKCBM	0	30	10	59	1
Fe series	Li_2O	K_2O	CdO	B_2O_3	Fe_2O_3
0LKCBF	30	0	10	59	1
10LKCBF	20	10	10	59	1
15LKCBF	15	15	10	59	1
20LKCBF	10	20	10	59	1
30LKCBF	0	30	10	59	1
Mn series	Li_2O	K_2O	ZnO	B_2O_3	MnO_2
0LKZBM	30	0	10	59	1
10LKZBM	20	10	10	59	1
15LKZBM	15	15	10	59	1
20LKZBM	10	20	10	59	1
30LKZBM	0	30	10	59	1
Fe series	Li_2O	K_2O	ZnO	B_2O_3	Fe_2O_3
0LKZBF	30	0	10	59	1
10LKZBF	20	10	10	59	1
15LKZBF	15	15	10	59	1
20LKZBF	10	20	10	59	1
30LKZBF	0	30	10	59	1

the strains. The structure of all the glasses was examined by means of X-ray diffraction using Phillips 1140 diffractometer, with Cu−Kα radiation ($\lambda = 1.5406$ Å). The diffractograms have been recorded in the Bragg angle region $0° \leq 2\theta \leq 80°$. The glass transition temperature, T_g was measured in all the glass samples using a temperature-modulated differential scanning calorimeter (TA Instruments, DSC 2910). All the samples were heated at the rate of 10 K/min in aluminum pans. The density of glass samples was measured by the standard principle of Archimedes using a sensitive microbalance and *o*-xylene as immersion liquid (density = 0.86 g/cm^3). At least, three samples of each glass were used to determine the density. The density is calculated according to the known formula,

$$D = \left[\frac{w_1}{(w_1 - w_2)} \times 0.86\right] \tag{3}$$

where w_1 is the weight of the sample in air, w_2 the weight of sample in xylene, and 0.86 is the density of xylene in g/cm^3. The measured values of density for the present glass samples are given in Table 2. Density values are precise to ±0.02 g/cm^3.

The molar volume of a given composition is calculated using the formula,

$$V_m = \frac{\sum_i M_i}{D} \tag{4}$$

where M_i denotes the molar mass of the glass given by $M_i = C_iA_i$. Here C_i and A_i are the molar concentration and the molecular weight of the *i*th component respectively. The molar volume is of higher interest, since it relates directly to the spatial distribution of the oxygen in the glass network. The data obtained on V_m for the prepared glass compositions are given in Table 2. As the concentration of K_2O (x) increases, in the glass system, a monotonic increase of the molar volume is seen.

Infrared transmission spectra of all the glass samples in KBr matrixes were recorded in the range 200−4000 cm^{-1} using a Perkin-Elmer 1600 IR spectrometer. Raman spectra were recorded at room temperature using a Jobin Yvon Labram HR800 spectrometer with a He−Ne laser (632.81

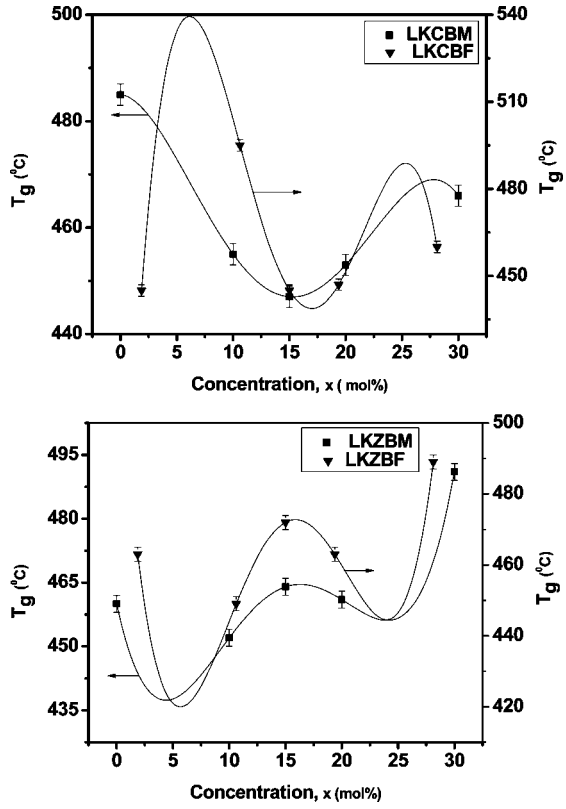

Figure 3. Compositional dependence of T_g of LKCBM, LKCBF, LKZBM, and LKZBF glasses.

nm) excitation line from a He−Ne laser. The spectra were collected in back scattering geometry with a resolution of 2 cm^{-1}.

TABLE 2: Density, Molar Volume, and Glass Transition Temperature of LKCBM, LKCBF and LKZBM, LKZBF Glass Systems

specimen	density (g/cm^3)	molar volume (g/mol)	T_g (°C)
LKCBM			
0	2.93	21.75	485
10	2.55	27.52	455
15	2.60	28.22	447
20	2.58	29.69	453
30	2.87	29.93	466
LKCBF			
0	2.94	21.88	445
10	2.60	27.27	495
15	2.59	28.61	445
20	2.61	29.63	453
30	2.80	29.91	466
LKZBM			
0	2.90	20.34	460
10	2.82	23.46	452
15	2.79	24.53	464
20	2.92	24.62	461
30	2.46	31.84	491
LKZBF			
0	2.38	25.11	463
10	2.40	27.58	449
15	2.43	28.56	472
20	2.41	29.14	463
30	2.61	30.29	489

3. Results and Discussion

(i) Results. The glasses under investigation were divided into four different groups: (1) LKCBM: $(30 - x)Li_2O - xK_2O - 10CdO - 59B_2O_3 - 1MnO_2$ $(0 \leq x \geq 30)$, (2) LKCBF:

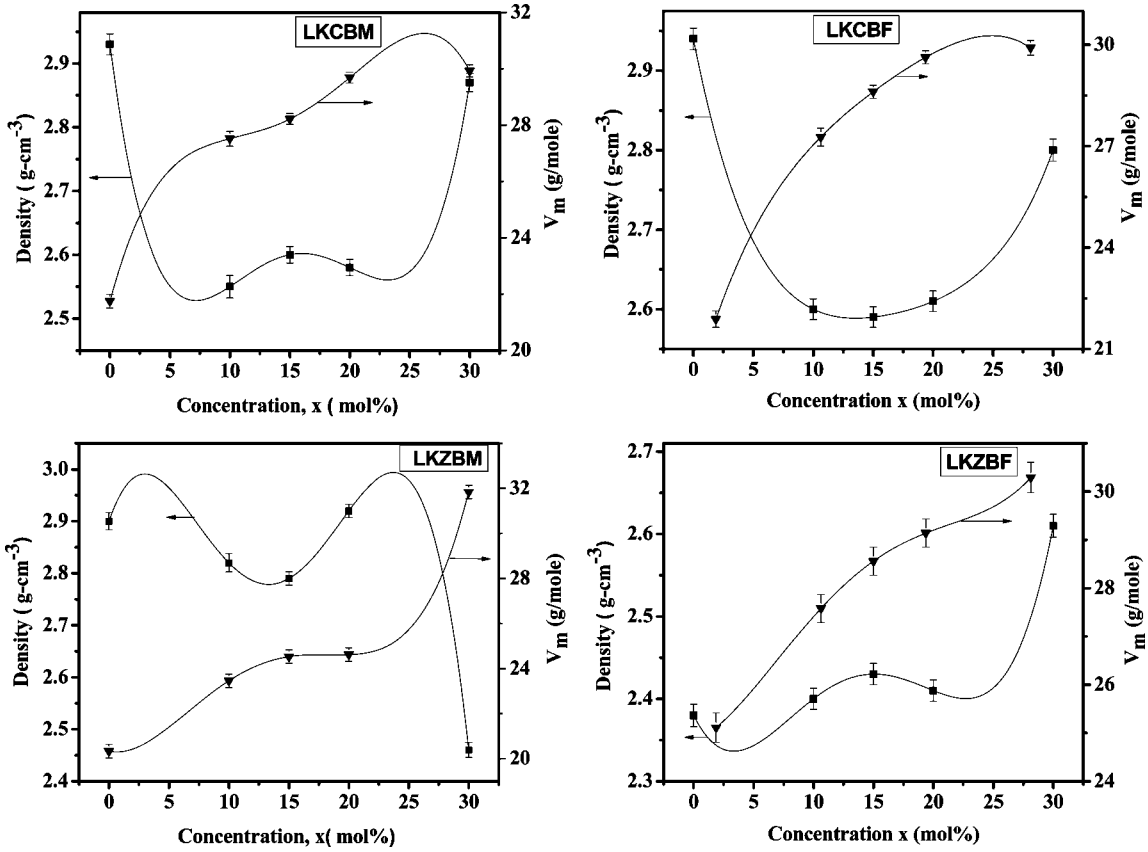

Figure 4. Compositional dependence of density and molar volume of LKCBM, LKCBF, LKZBM, and LKZBF glasses.

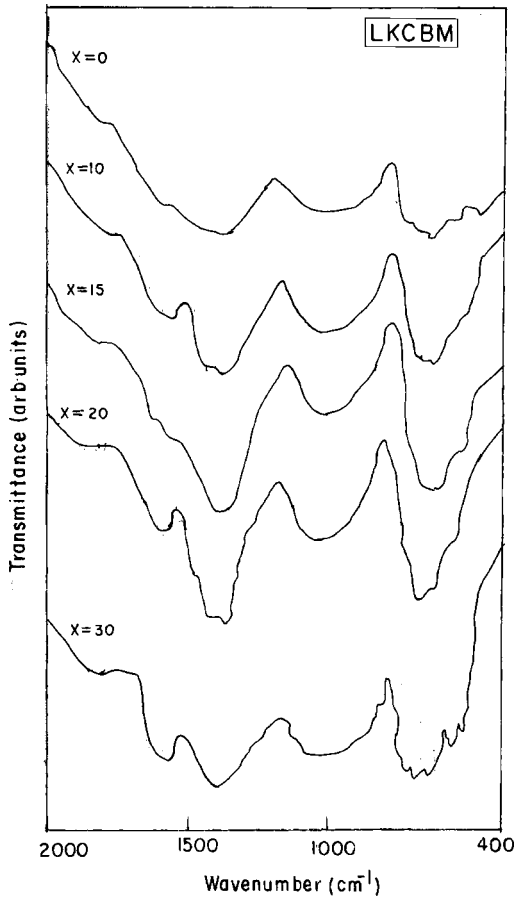

Figure 5. Room temperature IR transmission spectra of LKCBM glasses.

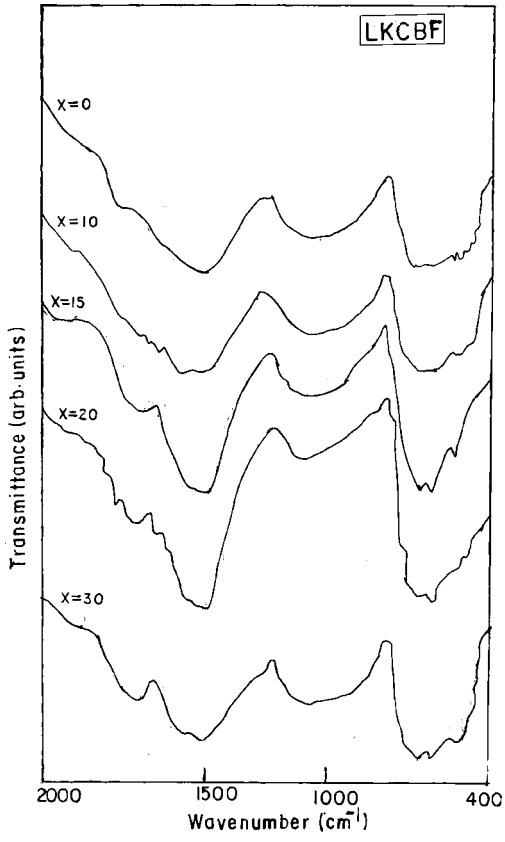

Figure 6. Room temperature IR transmission spectra of LKCBF glasses.

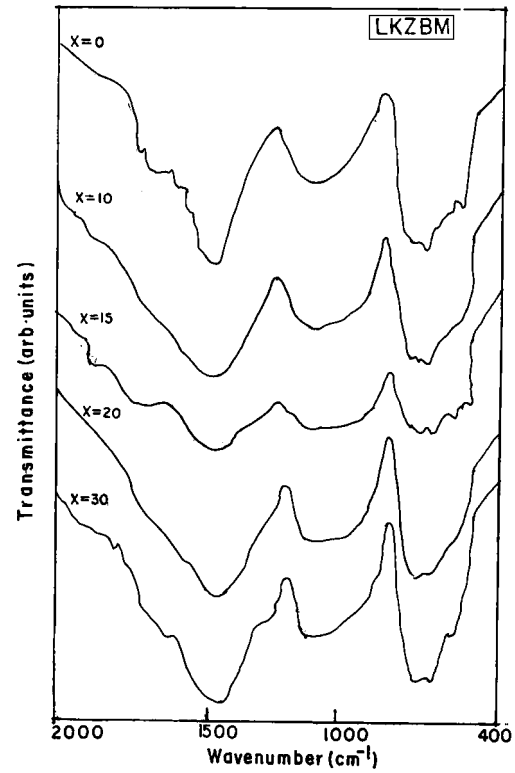

Figure 7. Room temperature IR transmission spectra of LKZBM glasses.

$(30 - x)Li_2O - xK_2O - 10CdO\ 59B_2O_3\ 1Fe_2O_3$ ($0 \leq x \leq 30$), (3) LKZBM: $(30 - x)Li_2O - xK_2O - 10ZnO - 59B_2O_3 - 1MnO_2$ ($0 \leq x \leq 30$); (4) LKZBF: $(30 - x)Li_2O - xK_2O - 10ZnO - 59B_2O_3 - 1Fe_2O_3$ ($0 \leq x \leq 30$). The compositions of glass samples are detailed in Table 1.

(a) X-ray Diffraction. X-ray diffraction (XRD) is a quite useful technique because it is possible to detect readily grown crystals in a glassy matrix. The X-ray diffraction pattern of an amorphous material is distinctly different from that of crystalline material and consists of a few broad diffuse haloes rather than sharp rings. XRD patterns of all the prepared glass samples depicted a diffused peak confirming the amorphous phase (vitreous state) of the glasses.

(b) Differential Scanning Calorimetry, Density, and Molar Volume. Differential scanning calorimetry (DSC) is used to characterize the glasses and to determine glass transition temperature (T_g). The DSC patterns of all the samples are shown in Figure 2. The value of T_g decreases with x and reaches a minimum around $x = 15$ and thereafter increases, indicating the presence of MAE in all the glass systems, as shown in Figure 3 (Table 2). The density is an important measure of the glass, and its value stands on its own as an intrinsic property capable of casting light on the short-range structure. The measured densities (D) of the present glass system along with evaluated values of molar volume (V_m) are given in Table 2. The composition dependence of density is shown in Figure 4. It is clear from the figure that the variation of density with composition is nonlinear, indicating the presence of mixed alkali effect (MAE) in these glass systems. The molar volume of the glasses increases with composition, showing no MAE (Figure 4). The molar volume will increase as a result of the creation of nonbridging oxygens (NBOs) which will break the bonds and increase spaces in the network.[19]

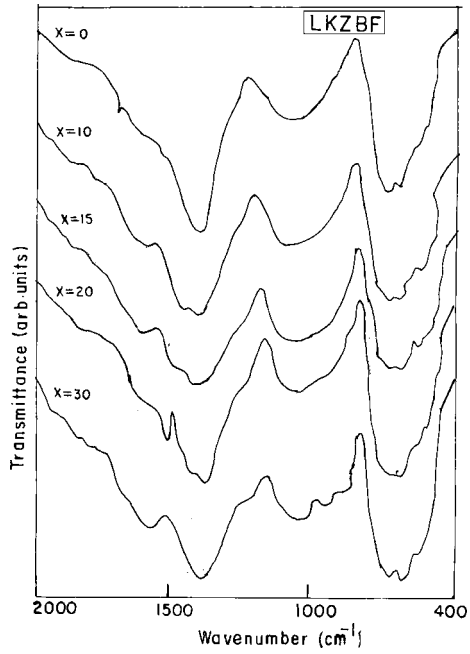

Figure 8. Room temperature IR transmission spectra of LKZBF glasses.

(c) IR Spectra. The transmission spectra of IR radiation gives information about molecular vibrations or rotation associated with a covalent bond. The IR spectra results because of a change in the dipole moment of the molecule. IR spectroscopy involves the twisting, bending, rotating, and vibrational motions in a molecule. Upon interaction with IR radiation, portions of the incident radiation are absorbed at particular wavelengths. This characterizes the functional groups comprising the molecule and the overall configuration of the atoms as well. The IR transmission spectra of LKCBM, LKCBF, LKZBM, and LKZBF glasses are given in Figure 5, Figure 6, Figure 7, and Figure 8, respectively. The assignments of the transmission bands as detected in the IR spectra are summarized in Table 3. The IR spectral data have been analyzed by comparing the experimental data of glasses with those of related crystalline compounds and vitreous B_2O_3.[20−22] In the analysis of IR spectra, only the mid-infrared region (400−1600 cm^{-1}), where the vibration of the B−O arrangements dominate, is considered. The spectra can be visually separated into three regions: (i) 400 − 780 cm^{-1} which is assigned to the bending vibrations of various borate arrangements, vibrations of Li cations through glass network, deformation modes of network structures as well as vibrations of some FeO_4 and MnO_4 groups; (ii) 780−1100 cm^{-1} is due to the B−O asymmetric stretching of tetrahedral BO_4 units and vibrations of diborates bridging to pentaborate groups; (iii) the strongest transmission band visible in the 1100−1600 cm^{-1} range is generated by the stretching vibrations of borate units in which boron atoms are connected to the three oxygens (BO_3 and B_3O_6 units).[19−23] Compositional dependence of the peak positions in the IR spectra corresponding to B−O−B bending vibrations (∼660 cm^{-1}) are shown in Figure 9 for LKCBM/LKCBF and LKZBM/LKZBF glasses, respectively.

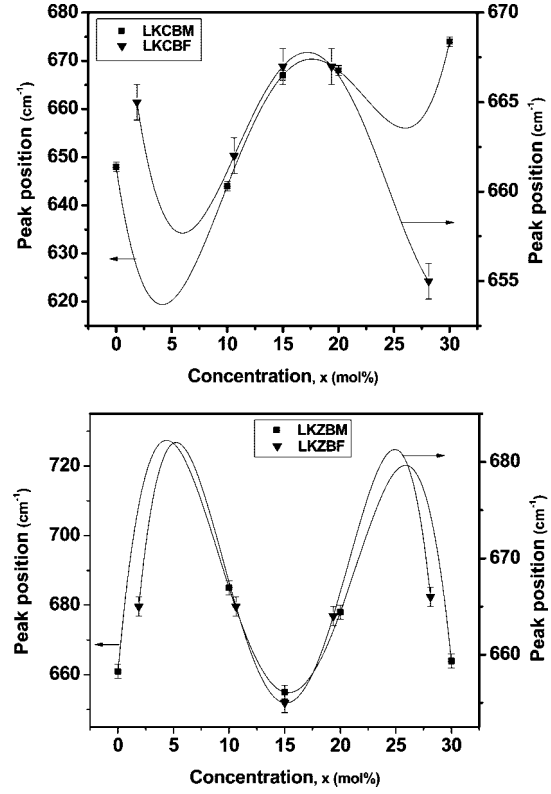

Figure 9. Compositional dependence of IR peak positions in the region 650−680 cm^{-1} of LKCBM and LKCBF glasses.

(d) Raman Spectra. Raman spectroscopy is one of the techniques which is often been utilized to investigate the structure of a melt. The room temperature Raman spectra of LKCBM, LKCBF, LKZBM, and LKZBF glass specimens in the region of 150−1600 cm^{-1} are shown in Figure 10, Figure

TABLE 3: Assignment of Infrared and Raman Bands in the Spectra of the LKCBM, LKCBF, LKZBM, and LKZBF Glass Systems

wave number (cm^{-1})			
IR	Raman	IR assignments	Raman assignments
∼ 460	∼470	O−B−O bond bending vibrations Li−O, K−O bond vibrations,	isolated diborate groups, Li−O, K−O bond vibrations
∼540		FeO_4 and MnO_4 bond vibrations	
∼680	∼660	B−O−B bond bending vibrations from pentaborate groups	pentaborate groups
∼760	∼765	BO_3−O–BO_4 bond-bending vibrations	symmetric breathing vibrations of six-member rings with one or two BO_3 triangles replaced by BO_4 tetrahedra
	∼960		Li−O−Fe/Mn, K−O−Fe/Mn vibrations
∼1013		pentaborate groups	
	∼1100		diborate groups
∼1235	∼1300	asymmetric stretching vibrations of B−O bonds from orthoborate groups	
∼1270			
∼1345	∼1345	asymmetric stretching modes of borate triangles BO_3 and BO_2O^-	BO_2O^- triangles linked to BO_4^- units
∼1480		asymmetric stretching modes of borate triangles BO_3 units	BO_2O^- triangles linked to other borate triangular units

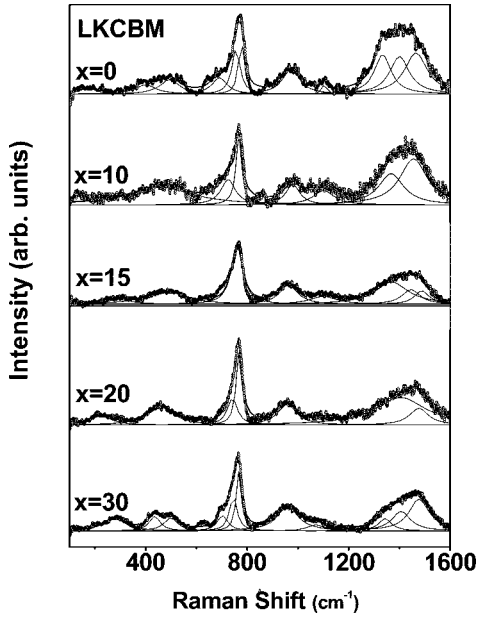

Figure 10. Room temperature Raman spectra of LKCBM glasses.

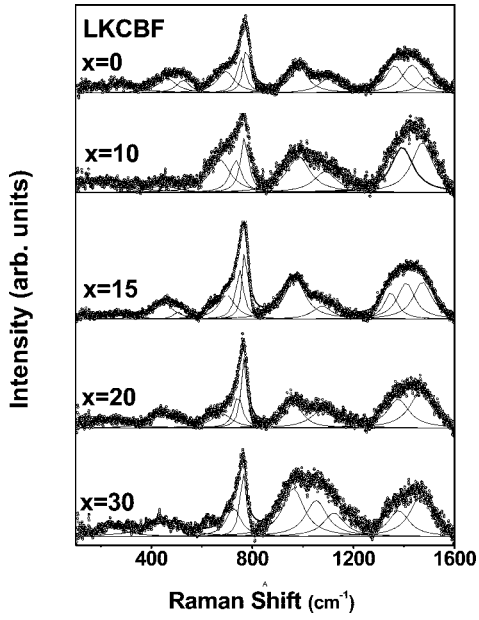

Figure 11. Room temperature Raman spectra of LKCBF glasses.

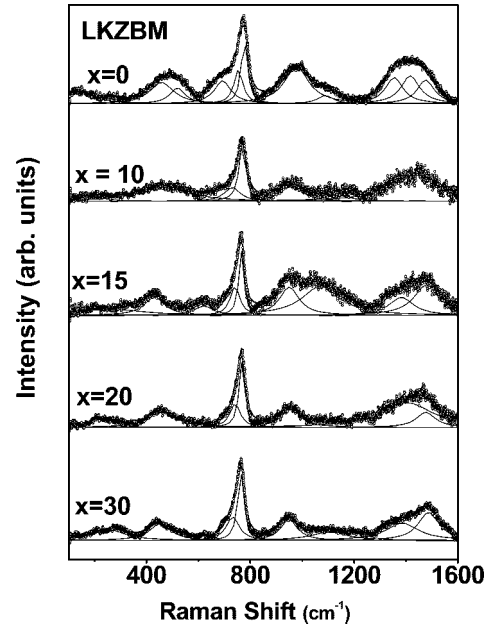

Figure 12. Room temperature Raman spectra of LKZBM glasses.

11, Figure 12, and Figure 13, respectively, and the band assignments of different bands is given in Table 3. There are four regions clearly visible in the spectra: (i) 190−600 cm^{-1}; (ii) 600−820 cm^{-1}; (iii) 900−1200 cm^{-1}; (iv) 1200−1600 cm^{-1}. In all the glasses studied the total alkali content is of 30 mol%. At this concentration of alkali content in borate glasses, the boroxol rings get converted mostly into pentaborate groups. This is observed clearly by the strong presence of peaks around 775, 650, 500 cm^{-1} and a weak peak ∼805 cm^{-1} resembling the localized breathing motions of oxygen atoms in the boroxol ring. The peak around 950 and 1110 cm^{-1} is due to diborate groups in the structure. The peaks in the high frequency region are due to the BO_2O^- triangles linked to BO_4 units and BO_2O^- triangles linked to other triangular units.[23,24]

(ii) Discussion. Borate-based glasses manifest a rich structural chemistry, and these boron structures are modified drastically with the addition of alkali oxide modifiers in the glass network. Besides alkali and alkaline earth oxides, several other oxide materials such as CdO, ZnO, PbO, and Ag_2O also act as stabilizing modifiers of the glass network. In the present study we have added 10 mol % CdO/ZnO to Li−K−B−Fe/Mn quaternary glasses by keeping total alkali concentration at 30%.

The 400−780 cm^{-1} spectral domain in the IR spectra is dominated by the absorption band centered at 680 cm^{-1} in the IR spectra. The intensity of this band is weak in LKCBM specimens, and the intensity and band position vary nonlinearly with alkali composition, indicating the mixed alkali effect (Figure 9). Further, this band is stronger in the case of ZnO-based glasses in all the specimens. The transmission signal in the regions 780−1200 cm^{-1} (N_4) and 1200−1600 cm^{-1} (N_3) reflect the content of tetrahedral ($B\varnothing_4^-$) and triangular ($B\varnothing_3$ and $B\varnothing_2O^-$) borate species, respectively (∅ represents an oxygen atom bridging two boron atoms). It is well-known that in borate glasses there is an isomerization process between three- and four-coordinated boron species as given below.

$$B\varnothing_2O^- \leftrightarrow B\varnothing_4^- \quad (5)$$

The relative variation in the intensity of bands representing N_4 and N_3 is nonlinear with the change in alkali concentration. In LKCBM glass specimens the N_3 bands are more intense than all the other glass specimens. It is evident from the graphs that Mn-doped glasses show stronger N_3 bands than Fe-doped samples. The N_4 band is quiet intense at $x = 30$ when compared to $x = 0$ samples, in all the glass systems. This suggests that the reaction 5 shifts to right, proving that the four-coordinated boron atoms are predominant in K-rich glasses.

Following the IR spectra, we can say that in the analyzed glasses, K-rich glasses show a strong N_4 band resembling four-coordinated boron in the glass network. compared to Li-rich glasses. The systematic mixing of Li−K in the present glasses manifests nonlinear changes in the intensity and position of IR bands.

In the Raman spectra of all the glassy specimens, there is a strong peak observed at ∼770 cm^{-1} which is characteristic of a six-membered ring with one or two BO_4 tetrahedra, and the peak at ∼808 cm^{-1}, which resembles a boroxol ring with BO_3 structures is not observed prominently. This suggests that at 30% alkali content the glass network is dominated by four-coordinated boron

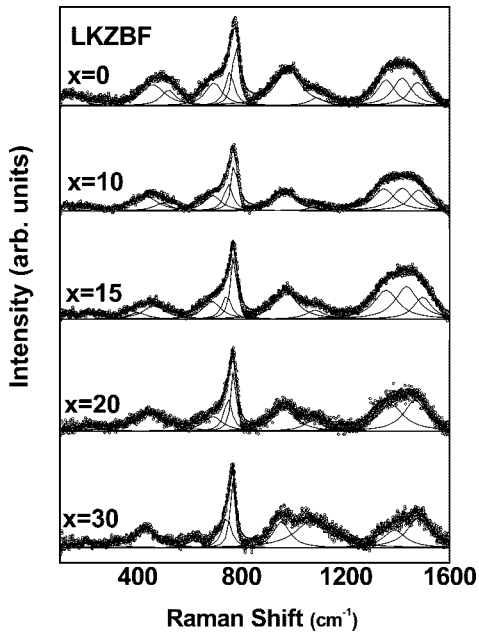

Figure 13. Room temperature Raman spectra of LKZBF glasses.

in the boroxol ring structures. The Raman spectra were deconvoluted into Lorentzian peaks using the least-squares method to identify the exact position of peaks and their intensity variation. The simultaneous occurrence of bands around 930, 770, 640, and 500 cm^{-1} is an indication of the presence of pentaborate groups in the borate glasses. Our experimental results indicate that all groups of glass specimens show these bands prominently.

The Raman bands in high frequency range have been assigned to the $B-O^-$ bonds attached to the large borate groups by Kamitsos et al.,[25] whereas it has been found that metaborate triangles linked to the BO_4^- tetrahedral exhibit their $B-O^-$ stretching activity at lower frequencies as a result of π-electronic interactions.[24] Thus, the spectral profile of the $B-O^-$ stretches can be used as an indirect probe of the BO_4^- units in the glass network. It is well-known that the network of pentaborate glasses is composed of borate arrangements containing BO_4^- tetrahedral and metaborate triangular units. As mentioned above in eq 5, there is isomerization between the three- and four-coordinated species, and one way of monitoring the equilibrium state in eq 5 is by measuring the intensity of Raman bands at 1380 and 1490 cm^{-1}. The ~1380 cm^{-1} Raman envelope is due to $B\varnothing_2O^-$ triangles linked to $B\varnothing$ units, while the 1490 cm^{-1} band is attributed to $B\varnothing_2O^-$ triangles linked to other borate triangular units. In the present study, the high frequency Raman spectra of all the glass specimens is fitted using two different Lorentzian convolutions, and the peak intensity variation is found to be nonlinear with the alkali content. The present results in quaternary glasses using Raman and IR spectroscopy are the first of their kind, and these nonlinear variations in the structural units (MAE) need further attention from both experimentalists and theorists.

4. Conclusions

The infrared and Raman spectral studies on the network structure of quaternary $Li-K-MO-B_2O_3$ glass systems doped with transition metal ions Mn^{2+} and Fe^{3+} have revealed the following conclusions.

(1) The TM ions Mn^{2+} and Fe^{3+} doped quaternary lithium potassium borate glasses have been prepared. The amorphous state of the prepared glasses was confirmed by X-ray diffraction spectra.

(2) Physical parameters such as density and molar volume are determined for all the glasses. The variation of density with the alkali content exhibits MAE. The glass transition temperatures of all the glass specimens are determined from the differential scanning calorimetric studies. All the glasses have a single glass transition temperature, and the variation of glass transition temperature with the alkali content is nonlinear, showing MAE.

(3) The IR spectra of all the glasses showed dramatic changes in the intensity of the bands in the regions (a) 780−1130 cm^{-1} and (b) 1200−1600 cm^{-1}. A nonlinear change with alkali content in the intensities of IR bands in these regions is observed. The various IR bands are assigned, and they are attributed to antisymmetric vibrations of B−O−B linkages, symmetric stretches, and bending vibrations of B−O−B linkages which are formed by sharing vertices of BO_4 tetraborate polyhedra.

(4) The Raman spectra of all the glasses exhibited several bands. These bands are attributed to BO_4 tetrahedra, the boroxol ring, and pentaborate groups linked to BO_4 tetrahedra. Further, the variation of intensities of some of the Raman bands with alkali content showed nonlinear variation (MAE). Also, there is isomerization between the three- and four-cocoordinated boron in the boroxol ring structures.

(5) The prime novelty of this work is for the first time the two complimentary spectroscopic techniques, IR and Raman, are employed to study the mixed alkali effect on the spectroscopic properties of multicomponent alkali borate glasses.

Acknowledgment. The authors thank the reviewers for their critical comments and useful suggestions. One of the authors G. Padmaja thanks AP Council for Science and Technology and University Grants Commission, Govt. of India, for providing partial financial assistance through merit research student fellowships. The authors also thank Dr. Vasant Sathe of UGC-DAE CSR, Indore, for providing experimental facilities.

References and Notes

(1) Kulkarni, A. R.; Lunkenheimer, P.; Loidi, A. *Mater. Chem. Phys.* **2000**, *63*, 93.
(2) Prabakar, S.; Mueller, K. T. *J. Non-Cryst. Solids* **2004**, *349*, 80.
(3) Krogh-Moe, J. *Phys. Chem. Glasses* **1962**, *101*, 46.
(4) Anderson, G.W.; Luchers, W. D. *J.Appl. Phys.* **1969**, *39*, 1634.
(5) Meera, B.; Ramakrishna, J. *J. Non-Cryst. Solids* **1993**, *159*, 1.
(6) Fouad, E.-D.; Fathy, A. A. W. *J. Appl. Phys.* **2006**, *100*, 093511.
(7) Hendrickson, J. R.; Bray, P. J. *Phys. Chem. Glasses* **1972**, *13*, 107.
(8) Van Ass, H. M.; Stevels, J. M. *J. Non-Cryst. Solids* **1974**, *14*, 131.
(9) Wan Gamert, W. J.; Stevels, J. M. *J. Non-Cryst. Solids* **1978**, *30*, 135.
(10) Matusita, K.; Takayama, S.; Sakka, S. *J. Non-Cryst. Solids* **1980**, *40*, 149.
(11) Keszel, D., King, R., Eds. In *Encyclopedia of Inorganic Chemistry*; John Wiley & Sons: New York, 1994; Vol. 11, p 318.
(12) Chryssikos, G.; Duffy, J.; Hutchinson, J.; Ingram, M.; Kamitsos, E.; Pappin, A. *J. Non-Cryst. Solids* **1994**, *172*, 378.
(13) Youngman, R. E.; Zwanziger, J. W. *J. Phys. Chem.* **1996**, *100*, 16720.
(14) Youngman, R. E.; Zwanziger, J. W. *J. Am. Ceram. Soc.* **1995**, *117*, 1397.
(15) Ulagaraj, S.; Rao, K. J. *Spectrochim. Acta* **1984**, *40*, 1081.
(16) Jellison, G. E.; Panek, L. W.; Bray, P. J.; Rouse, G. B. *J. Chem. Phys.* **1977**, *66*, 802.
(17) Bamford, C. R. *Phys. Chem. Glasses* **1962**, *3*, 189.
(18) Wong, J.; Angell, C. A. *Glass Structure by Spectroscopy*; Marcel Dekker: New York, 1976.
(19) Duffy, J A.; Ingram, M. D. *J. Inorg. Nucl. Chem.* **1975**, *37*, 1203.
(20) Condrate, R. A. *J. Non-Cryst. Solids* **1986**, *84*, 26.
(21) Raluca, C.-L.; Ioan, A. *J. Non-Cryst. Solids* **2007**, *353*, 2020.
(22) Tetsuji, Y.; Noboru, K.; Shuichi, S.; Masayuki, Y. *J. Non-Cryst. Solids* **2003**, *321*, 147.
(23) Ryichi, A.; Norikazu, O.; Norimasa, U. *J. Non-Cryst. Solids* **2001**, *293*, 471.
(24) Chryssikos, G. D.; Kamitsos, E. I.; Patsis, A. P.; Bitsis, M. S.; Karakassides, M. A. *J. Non-Cryst. Solids* **1990**, *126*, 42.
(25) Kamitsos, E. I.; Karakassides, M. A.; Chryssikos, G. D. *J. Phys. Chem.* **1987**, *91*, 1073.

JP809318E